Original article

In vitro and *in silico* analysis of *Solanum torvum* fruit and methyl caffeate interaction with cholinesterases

Maha Aljabri [a],[*], Khadiga Alharbi [b], Mona Alonazi [c]

[a] *Department of Biology, Faculty of Applied Science, Umm Al-Qura University, Makkah, Saudi Arabia.*
[b] *Department of Biology, College of Science, Princess Nourah bint Abdulrahman University, P.O. Box 84428, Riyadh 11671, Saudi Arabia*
[c] *Biochemistry Department, College of Science, King Saud University, Riyadh 11495, Saudi Arabia*

A B S T R A C T

Oxidative stress along with dysfunction in cholinergic neurotransmission primarily underlies cognitive impairment. A significant approach to mitigate cognitive dysfunction involves the inhibition of cholinesterases, namely acetylcholinesterase (AChE) and butyrylcholinesterase (BChE). Exploring the potential antioxidant and anticholinesterase effects of edible plants holds promise for their utilization as botanicals to enhance cognition. *Solanum torvum* fruit with vast biological properties are used as food. In the present study, butanolic extract of *S. torvum* fruits (BESTF) was prepared. Additionally, the study investigated into the properties of methyl caffeate (MC), a compound present in *S. torvum*, obtained in its pure form. *In vitro* antioxidant and anticholinesterases activity of BESTF and MC were determined. BESTF and MC showed potent antioxidant property. BESTF and MC dose-dependently inhibited AChE (IC$_{50}$ values: 166.6 µg/ml and 680.6 µM, respectively) and BChE (IC$_{50}$ values: 161.55 µg/ml and 413 µM, respectively). BESTF and MC inhibited AChE and BChE in competitive mode. Active site gorge of AChE/BChE was occupied by MC which formed interaction with amino acids present in catalytic site and PAS in *in silico*. Further, molecular dynamics simulations followed by free energy calculation, principal component analysis and dynamic cross-correlation matrix provided the compelling evidence that that MC maintained stable interactions during MD simulation with AChE and BChE. Collectively, the results from the present study underlines the cognitive-enhancing effect of BESTF and MC.

© 2023 The Author(s). Published by Elsevier B.V. on behalf of King Saud University. This is an open access article under the CC BY-NC-ND license (http://creativecommons.org/licenses/by-nc-nd/4.0/).

1. Introduction

Cholinergic enzymes acetylcholinesterase (AChE) and butyrylcholinesterase (BChE) are involved in the catalytic hydrolyzation of neurotransmitter acetylcholine (ACh) thereby in cholinergic neurotransmission. However, under Alzheimer's disease (AD; one of the neuronal disorders) conditions, the cholinergic neurons are selectively lost as well as level of ACh is decreased due to which learning and memory are impaired (Chen et al., 2022). Hence, inhibition of AChE and BChE is considered for symptomatic treatment of AD (Darvesh, 2016; Marucci et al., 2021). Apart from dysfunction in cholinergic neurotransmission, amyloid β (Aβ) peptide accumulation and increased oxidative stress is involved in the progression of neuronal damage under AD conditions (Butterfield and Boyd-Kimball, 2018). BChE and AChE is associated with Aβ peptide in AD brain and speculated to aggregate Aβ peptide (Mushtaq et al.,

2014). Also, AChE-Aβ complex is highly toxic in comparison to Aβ alone under AD conditions (Dinamarca et al., 2010). At present, the inhibitors of AChE and BChE such as rivastigmine, galantamine, and donepezil are approved for AD treatment by Food and Drug Administration, USA (Yiannopoulou and Papageorgiou, 2020). However, these drugs have shortcomings such as low bioavailability and several side-effects (hepatotoxicity and gastrointestinal adverse effects) (Yiannopoulou and Papageorgiou, 2020). Hence identification of compounds that inhibits these enzymes (AChE and BChE) and also have potential to overcome oxidative stress through antioxidant activity would be advantageous in the AD treatment.

Numerous medicinal plants have been reported for its potential to inhibit AChE and BChE. Some examples for these medicinal plants are *Terminalia chebula*, *Ulva reticulate*, *Terminalia bellerica*, *Acacia catechu*, *Illicium verum*, *Avicennia officinalis*, *Hemidesmus indicus*, *Bacopa monniera*, *Ginkgo biloba*, *Clivia miniata*, *Centella asiatica*, *Stemona collinsiae*, *Caesalpinia ferrea*, *Nelsonia canescens*, *Amaryllis belladonna*, *Cassia fistula*, *Senna pendula*, *Tussilago farfara* and *Crinum jagus* (Patel et al., 2018). Accordingly, present study

---

evaluates the anticholinesterases activities of *Solanum torvum* fruit. *S. torvum* (common name: Turkey berry) is an important vegetable in the market which belongs to the family of *Solanaceae*. The leaves and fruits of *S. torvum* were reported for several biological activities such as anticancer, antimicrobial, antioxidant, analgesic and cardioprotective activity (Darkwah et al., 2020; Senizza et al., 2021; Sani et al., 2022). The phytochemical profile from *S. torvum* exhibited that alkaloids, flavonoids, saponins, phenols, tannins and glycosides are present in adequate level. Presence of phenolic compounds such as kaempferol 3-O-glucosyl-rhamnosyl-galacto side, p-coumaric acid, DL-proline 5-oxo-methyl ester, quercetin, salicylic acid, myricetin glucosides, butylated hydroxytoluene, rutin, nepetin, caffeic acid, gallic acid, pyrogallol, catechin mullein, genistein, scutellarein, and rhoifolin in *S. torvum* have been reported (Senizza et al., 2021; Sani et al., 2022). Although many compounds have been identified in *S. torvum* fruit, the biological property of methyl caffeate (MC) isolated from *S. torvum* has been widely studied and reported for its mammalian glucosidase inhibitory activity, antidiabetic activity, antimicrobial, antimycobacterial and anticancer activity (Takahashi et al., 2010; Gandhi et al., 2011; Balachandran et al., 2015). Also, it has shown that MC protected the neuronal (hippocampus) cells against glutamate and hydrogen peroxide (H_2O_2)-induced toxicity by increasing the level of endogenous antioxidant glutathione and decreasing the accumulation of reactive oxygen species (ROS) (Ishige et al., 2001). Based on these existing biological potential of *S. torvum* fruits and MC, the present work evaluated the inhibitory effect of butanolic extract of *S. torvum* fruits (BESTF) and MC on cholinesterases (AChE and BChE). Type of inhibition and inhibitory constant (Ki) of BESTF and MC was determined by kinetic analysis. The interaction between MC

and human AChE/BChE was elucidated via computational molecular docking analysis. Subsequent to this, molecular dynamics (MD) simulation was employed to ascertain the stability of the binding between MC and AChE/BChE. To gain insights into the interaction between MC and the proteins (AChE and BChE), post-MD analyses including Molecular Mechanics with Generalised Born and Surface Area Solvation (MM/GBSA), Principal Components Analysis (PCA), and Dynamic Cross-Correlation Matrix (DCCM) analysis were performed. Furthermore, the *in vitro* scavenging activities against free radicals of both BESTF and MC were also determined.

2. Materials and methods

2.1. Materials

MC was purchased from TCI Chemicals (Japan). All other chemicals were purchased from Sigma (USA).

2.2. Extraction of S. torvum fruits

Fresh *S. torvum* fruits were cleaned using water, then dried under shadow and ground. The dried powder (10 g) was extracted at room temperature using methanol (200 ml) by maceration for 48 h. The supernatant obtained after centrifugation at 9000 rpm for 20 min was pooled and fractioned using hexane in separating funnel. After hexane extraction, the methanolic extract was sequentially fractionated using n-butanol. The phytochemicals precipitated after the addition of n-butanol was collected and air dried. The air-dried fraction was used for further biological activity and named as BESTF.
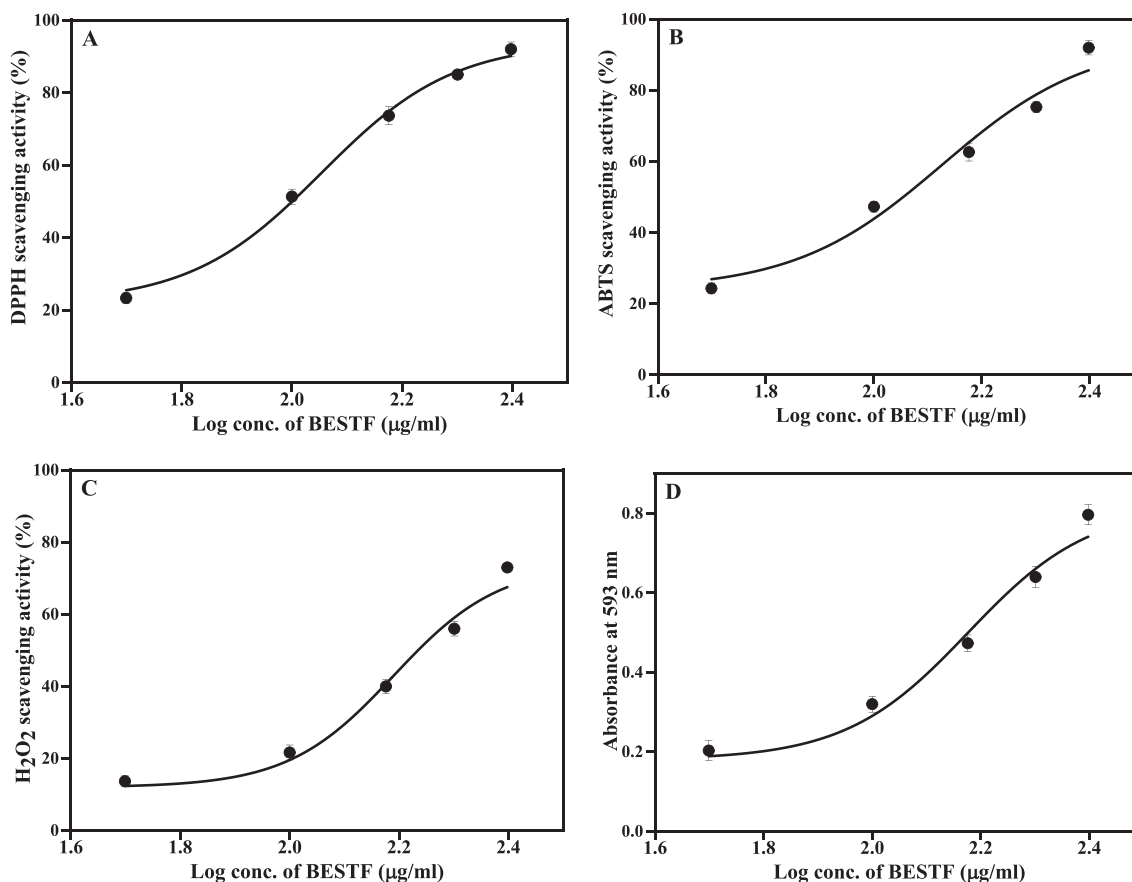
Fig. 1. BESTF antioxidant activity. Scavenging of (A) DPPH, (B) ABTS and (C) H_2O_2 radicals. (D) FRAP activity.

2.3. Phytochemicals quantification

The total flavonoids content (TFC) and total phenolic content (TPC) of the sample were determined using the aluminium chloride reagent method and Folin-Ciocalteau reagent method, following the protocol outlined earlier (Al-Masri and Ameen, 2023). The amount of saponin present in the sample was determined using the vanillin reagent method, following the procedure outlined earlier (Hiai et al., 1976). The tannin content was measured using the Folin-Ciocalteau reagent method as mentioned earlier (Galvão et al., 2018). The TPC, TFC, saponin and tannin reported as gallic acid (GA) equivalent (mg GAE/g of BESTF), quercetin equivalent (mg QE/g of BESTF), diosgenin equivalent (mg DGE/g of BESTF) and tannic acid equivalent (mg TAE/g of BESTF), respectively.

2.4. In vitro antioxidant activity

BESTF and MC antioxidant activities were determined using various assays such as scavenging of radicals [1, 1-diphenyl-2-picrylhydrazyl (DPPH), 2,2′-azino-bis(3-ethylbenzothiazoline-6-sulphonic acid) (ABTS), hydrogen peroxide (H_2O_2)] and ferric reducing antioxidant power (FRAP) (Pavithra and Vadivukkarasi, 2015; Al-Masri and Ameen, 2023). For antioxidant assays, various concentrations of BESTF (50–250 μg/ml) or MC (1–5 μM) were used. At the end of the assays, the absorbances were read using UV–visible microplate reader (BioTek Epoch 2, Agilent, USA).

2.5. AChE and BChE enzyme activity assay

Electric eel AChE was used as procured and BChE was prepared as described earlier. Also, further the enzyme assay was carried out as mentioned in the previous study "The reaction mixture of enzyme assay consisted for 100 mM of potassium phosphate (KPO_4) buffer (pH 7), aliquot of enzyme (electric eel AChE or human serum BChE), respective substrates and 2 mM of 5, 5′-Dithio-bis (2-Nitrobenzoic acid). For AChE and BChE assay, 1 mM acetylthiocholine iodide (ATCI) and 3 mM butyrylthiocholine iodide (BTCI) was used as substrate, respectively. The total assay mixture was allowed to incubated at 37 °C for 10 min and 5 min for AChE and BChE assay, respectively. The chromophore was read at 412 nm" (Sakayanathan et al., 2019).

2.6. Enzyme inhibition assay

AChE and BChE enzyme activity inhibition was determined in the presence of various concentrations of BESTF (50–250 μg/ml) or MC (250–1250 μM for AChE and 100–500 μM for BChE) in 2 mM KPO_4 buffer (pH 7). The tube without BESTF or MC served as control. The residual activity after incubation was measured as mentioned above. All the assays were carried out in triplicate and the average of the obtained values was taken for analysis.

2.7. Kinetics of AChE inhibition

The enzyme kinetic assays were performed to determine the mode of inhibition [using Lineweaver and Burk double reciprocal plot (LB plot)] and inhibitor constant (using Dixon plot). AChE and BChE assays were performed using various concentrations of substrates (0.4 mM − 1 mM of ATCI for AChE and 1.2 mM–3 mM BTCI for BChE) in the absence and in the presence of BESTF (50–200 μg/ml) or MC (250–1000 μM for AChE and 100–400 μM for BChE) (Lineweaver and Burk, 1934; Dixon, 1953).
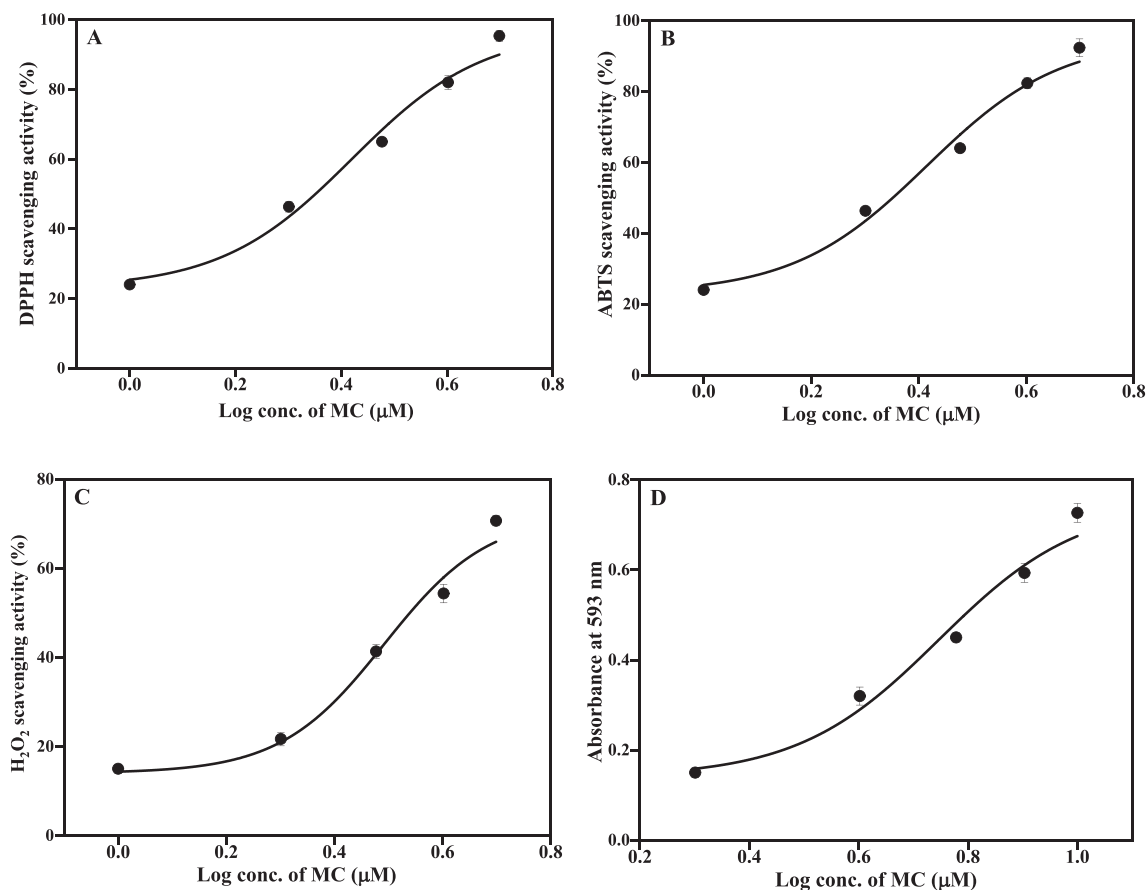
Fig. 2. MC antioxidant activity. Scavenging of (A) DPPH, (B) ABTS and (C) H_2O_2 radicals. (D) FRAP activity.

2.8. In silico analysis

2.8.1. Molecular docking study

Human BChE (PDB code: 1P0I) (Nicolet et al., 2003) and human AChE (PDB code: 4EY6) (Cheung et al., 2012) crystal structures were obtained. The docking of MC with AChE and BChE was performed using induced fit docking (IFD) approach with extra precision (XP) method. This docking procedure was carried out utilizing the Schrödinger suite 2018 software package.

2.8.2. Molecular dynamics simulation

Molecular dynamics (MD) simulation was conducted for 100 ns using the OPLS4 force field, which was implemented in the Desmond package as described previously (Chitra et al., 2022).

2.9. PCA and DCCM analysis

DCCM and PCA were employed to assess the essential dynamics, representing the crucial motions necessary for protein functionality and the residual displacement observed in the docked complex throughout the MD simulation over time. These calculations were conducted using CPPTRAJ and an R package, following methods described in previous studies (Roe and Cheatham, 2013).

3. Results

3.1. Phytochemical characterization of BESTF

The concentration of TPC and TFC was found to be 36.32 ± 1.9 2 mg GAE/g of BESTF and 68 ± 1.68 mg QE/g of BESTF, respectively. The concentration of saponin was found to be 92.5 ± 2.12 mg DGE/g of BESTF. The concentration of tannin was found to be 196.5 ± 4. 6 mg TAE/g of BESTF.

3.2. Antioxidant activity

BESTF revealed potent scavenging effect against DPPH, ABTS and H_2O_2 in dose-dependent manner. BESTF showed highest scavenging activity against DPPH (Fig. 1A) with the IC_{50} values of 113.35 µg/ml in comparison with ABTS scavenging (Fig. 1B) with the IC_{50} values of 133.55 µg/ml. Further, BESTF exhibited H_2O_2 scavenging activity (Fig. 1C) and IC_{50} was found to be 154.97 µg/ml. In addition, FRAP result of BESTF showed linear increase in FRAP activity with the concentration ranging from 50 to 250 µg/ml (Fig. 1D). Similarly, MC showed concentration-dependent scavenging activity. However, MC showed powerful antioxidant activity at low micromolar concentrations. For DPPH, ABTS and H_2O_2 scavenging activities, the IC_{50} value for MC was found to be
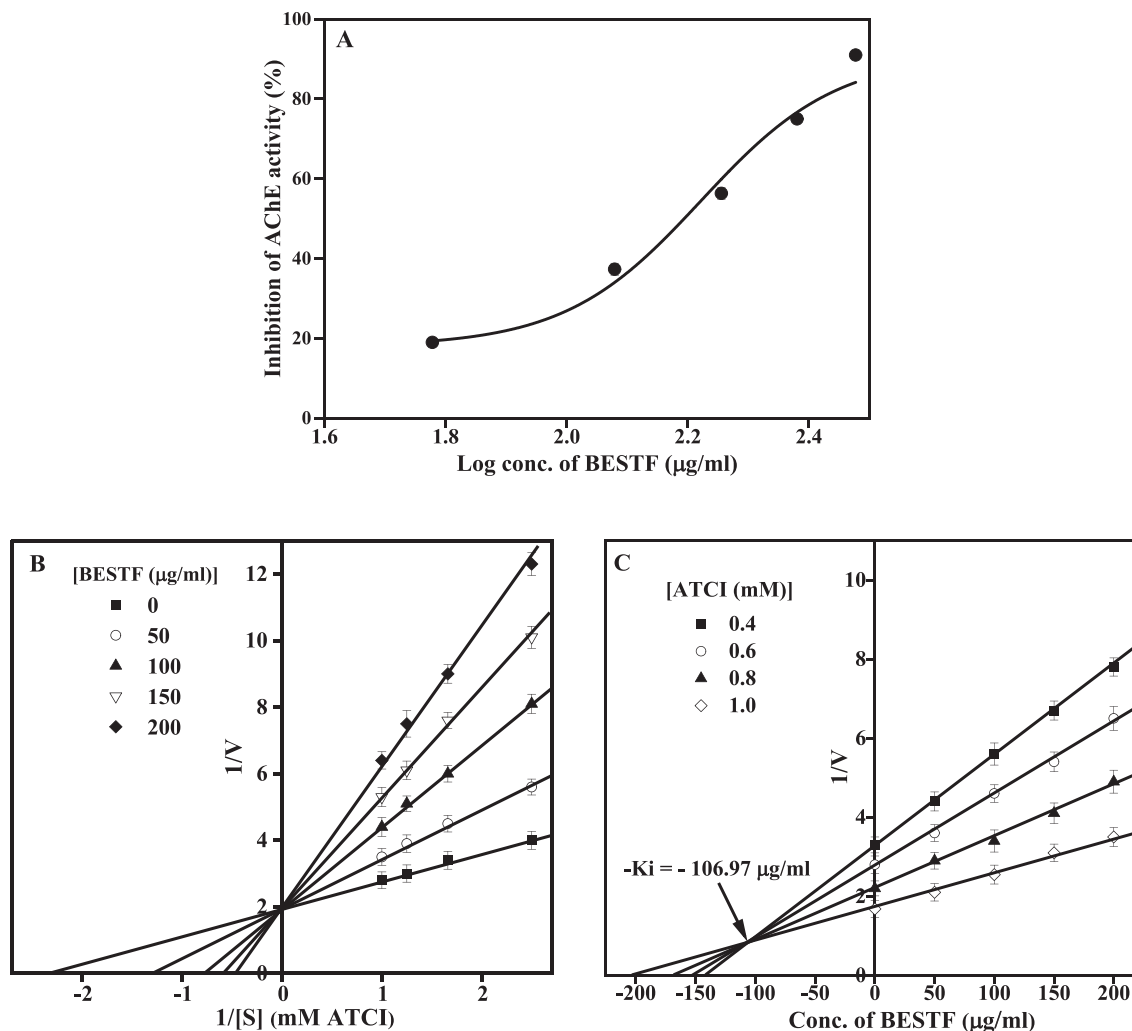
Fig. 3. BESTF effect on AChE enzyme activity. (A) BESTF inhibition of AChE enzyme. (B) LB plot showing the inhibition type. (C) Dixon plot with Ki value of BESTF for AChE enzyme activity.

2.62 µM, 2.59 µM and 3.10 µM, respectively (Fig. 2A, 2B and 2C). Further, MC showed higher FRAP activity (Fig. 2D) in concentration-dependent manner.

3.3. Inhibition of AChE and BChE by BESTF and MC

BESTF exhibited AChE and BChE inhibition in concentration-dependent manner (Figs. 3A and 4A). BESTF inhibited AChE and BChE competitively (LB plot; Figs. 3B and 4B). The IC$_{50}$ value of BESTF against AChE and BChE was found to be 166.6 µg/ml and 161.55 µg/ml. The Ki value of BESTF against AChE and BChE was found to be 106.97 µg/ml (Fig. 3C) and 150.87 µg/ml (Fig. 4C). Also, MC inhibited AChE and BChE dose-dependently (Figs. 5A and 6A). Similar to BESTF, MC inhibited the enzymes competitively (Figs. 5B and 6B). The IC$_{50}$ value of MC against AChE and BChE was found to be 680.6 and 291.6 µM, respectively. The Ki value of MC against AChE and BChE was found to be 366.16 µM (Fig. 5C) and 190.39 µM (Fig. 6C), respectively.

3.4. MC interaction with AChE and BChE

3.4.1. Molecular docking and molecular dynamics analysis

The docking score for MC with AChE and BChE was found to be −8.43 kcal/mol and −8.68 kcal/mol, respectively. MC interaction with AChE during docking and after MD simulation is shown in Fig. 7. The superimposed structure of MC interaction with AChE

at the end of docking and after simulation is given in Fig. 7A. MC occupied the AChE active site and formed stable interaction throughout the MD simulation. MC hydrogen bonded with amino acids such as Trp86, Asn87, Tyr124, Glu202 and Ser203 at the end of docking. Also, hydrophobic interactions were formed with amino acids Gly120 (pi-stack-pi-orbital) and, Gly121(pi-stack-pi-orbital) (Fig. 7B and Table 1). After MD simulation, new interactions were formed by MC with Asp74, Thr83, Ser125 and His447. Also, MC's contact with amino acids, Trp86 and Ser203 was maintained similar to docking. Hydrophobic interactions were formed with Val73 (alkyl-alkyl) and Trp86 (pi-orbital-pi-orbital) (Fig. 7C and Table 1). The interaction between MC and amino acids present in AChE throughout 100 ns MD trajectory is shown in Fig. 7D. MC stably interacted with His447, which is a catalytic amino acid throughout the simulation.

Superimposed structure of MC interaction with BChE at the end of docking and 100 ns MD simulation is shown in Fig. 8A. Similar to AChE, MC formed stable interaction within BChE active site space. MC hydrogen bonded with Tyr128, Glu197, Tyr332, Met437 and His438 of BChE (Fig. 8B). In addition, MC formed hydrophobic interaction with Trp82 (pi-orbital-pi-orbital) and Ala328 (pi-orbital-alkyl). At the end of simulation, MC interacted with the following amino acids present in the BChE such as Gly116, Ser198, Ala328, His438 and Gly439 (Fig. 8C). In addition, MC hydrophobically interacted with Ala328 (pi-orbital-alkyl) and His438 (pi-orbital-pi-orbital) of BChE. The detail of MC interaction with amino
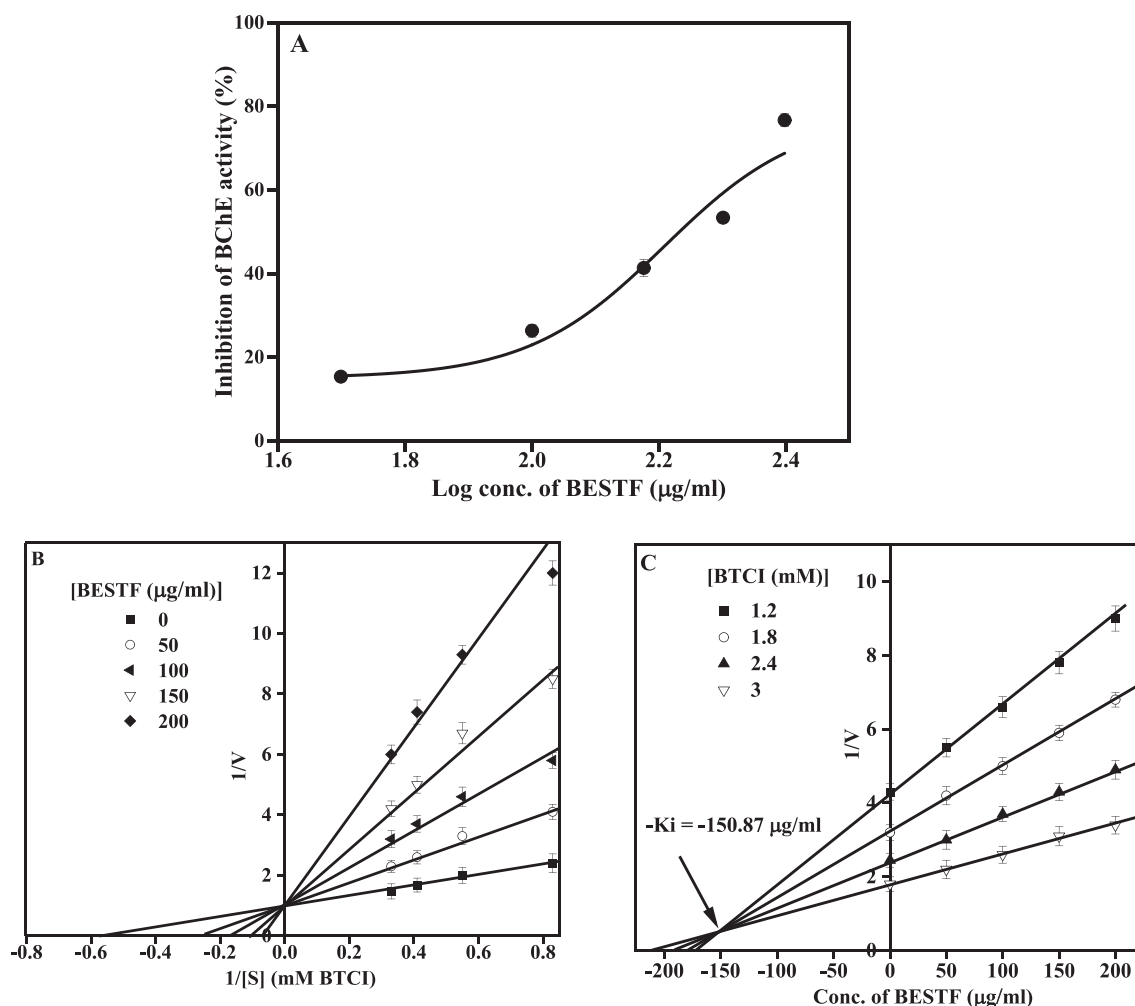
Fig. 4. BESTF effect on BChE enzyme activity. (A) Inhibition of BESTF against BChE enzyme. (B) LB plot showing the inhibition type. (C) Dixon plot with Ki value of BESTF for BChE activity.
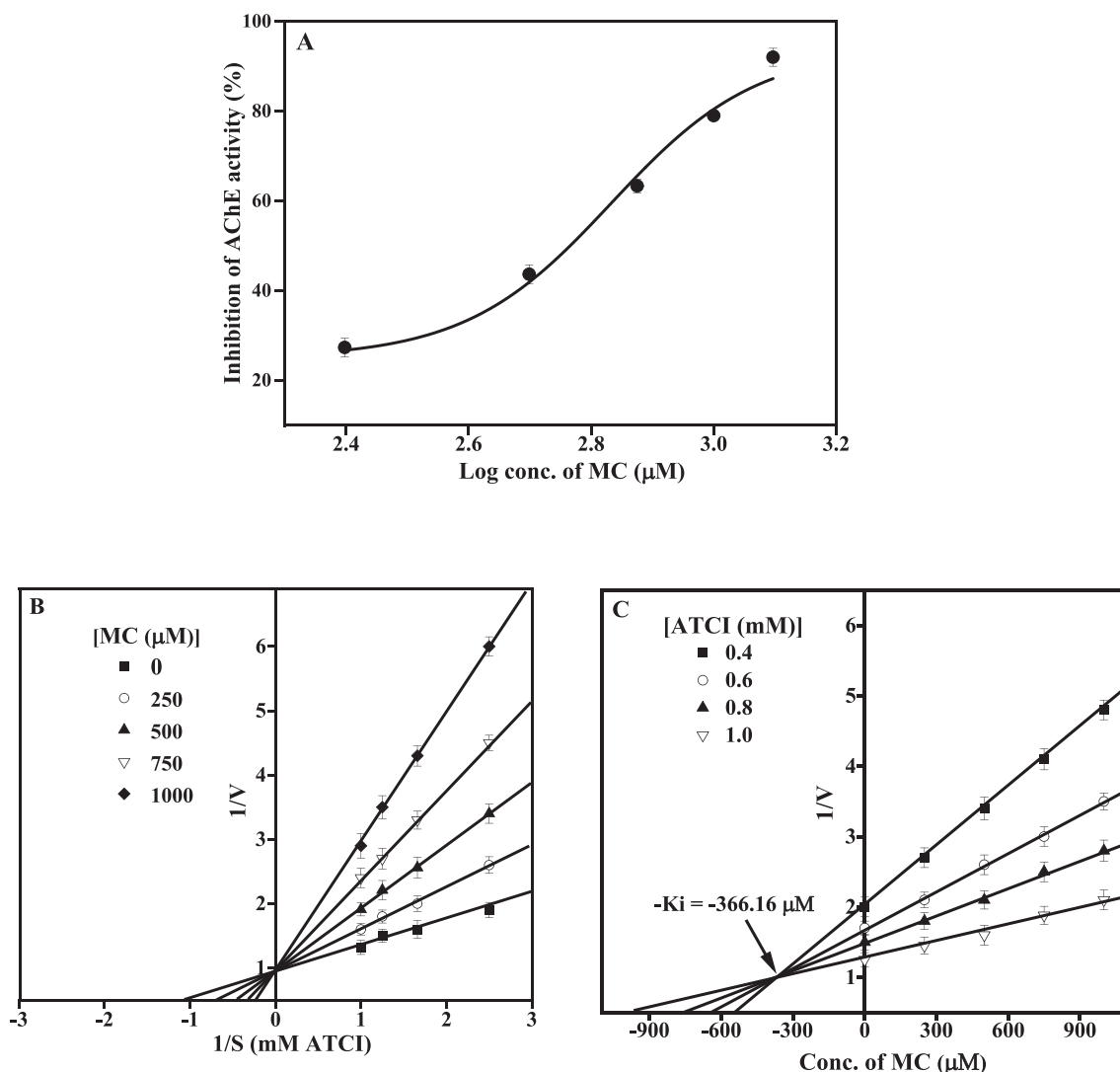
Fig. 5. MC effect on AChE enzyme activity. (A) Inhibition of MC against AChE enzyme. (B) LB plot showing inhibition type. (C) Dixon plot with Ki value of MC for AChE activity.

acids of BChE throughout 100 ns MD trajectory is shown in Fig. 8D. MC has formed stable contact with His438 (catalytic amino acid) through hydrophobic bond during the simulation.

The difference in Root mean square deviation (RMSD) values during MD simulation for both AChE and BChE with MC (Fig. 9A and 9B) were within 1.5 Å range which shows that, both complexes maintained the stable binding throughout 50 ns simulation time. Followed by, Root mean square fluctuation (RMSF) was used to find the amino acid's flexibility present in the N and C-terminal, alpha helix, β-sheet and loop region of the enzyme. RMSF results of both AChE and BChE with MC (Fig. 9C and 9D) has shown less flexibility and more rigidity between catalytic site amino acids region which indicated that, both complexes are stable during 100 ns simulation. The aromatic amino acids positioned in acyl binding pocket of both the proteins (AChE and BChE) have shown fluctuations due to binding of MC.

3.4.2. Binding free energy estimation

MM/GBSA calculations showed that the ΔG of AChE and BChE as −41.85 and −8.49 kcal/mol, respectively (Table 2). During the MD simulation, the firm binding of MC with AChE as well as BChE was facilitated by three main factors: Van der Waals force, lipophilic energy, and Coulomb's energy. These intermolecular forces

played a significant role in ensuring the strong and stable interaction between MC and the enzymes AChE and BChE throughout the simulation.

3.4.3. PCA and DCCM analysis

In the PCA graph of the MC-AChE complex (Fig. 10A), the eigenvalues of the proteins were plotted against their corresponding eigenvector indices. The first five eigenvectors displayed dominant movements with higher eigenvalues, accounting for 20.5% to 55.7% of the total variance. Beyond the fifth eigenvector, the eigen fraction reached a static elbow point, indicating that subsequent eigenvectors showed no significant variations. PC1 clusters exhibited the highest variability, representing 20.41% of the total variance, followed by PC2 with 11.68% variability, and PC3 with minimal variability of 6.58%. The lower variability in PC3 suggests a more steadied protein–ligand binding, occupying a smaller region in the phase space and resulting in a more compact structure. In all clusters, conformational changes are present [blue regions: significant movements; white regions: intermediate movements; red regions: less flexibility].

In the cross-correlation map (Fig. 10B), the pairwise correlation between MC and the AChE protein was shown using pairwise cross-correlation coefficients. Residues with correlation coeffi-
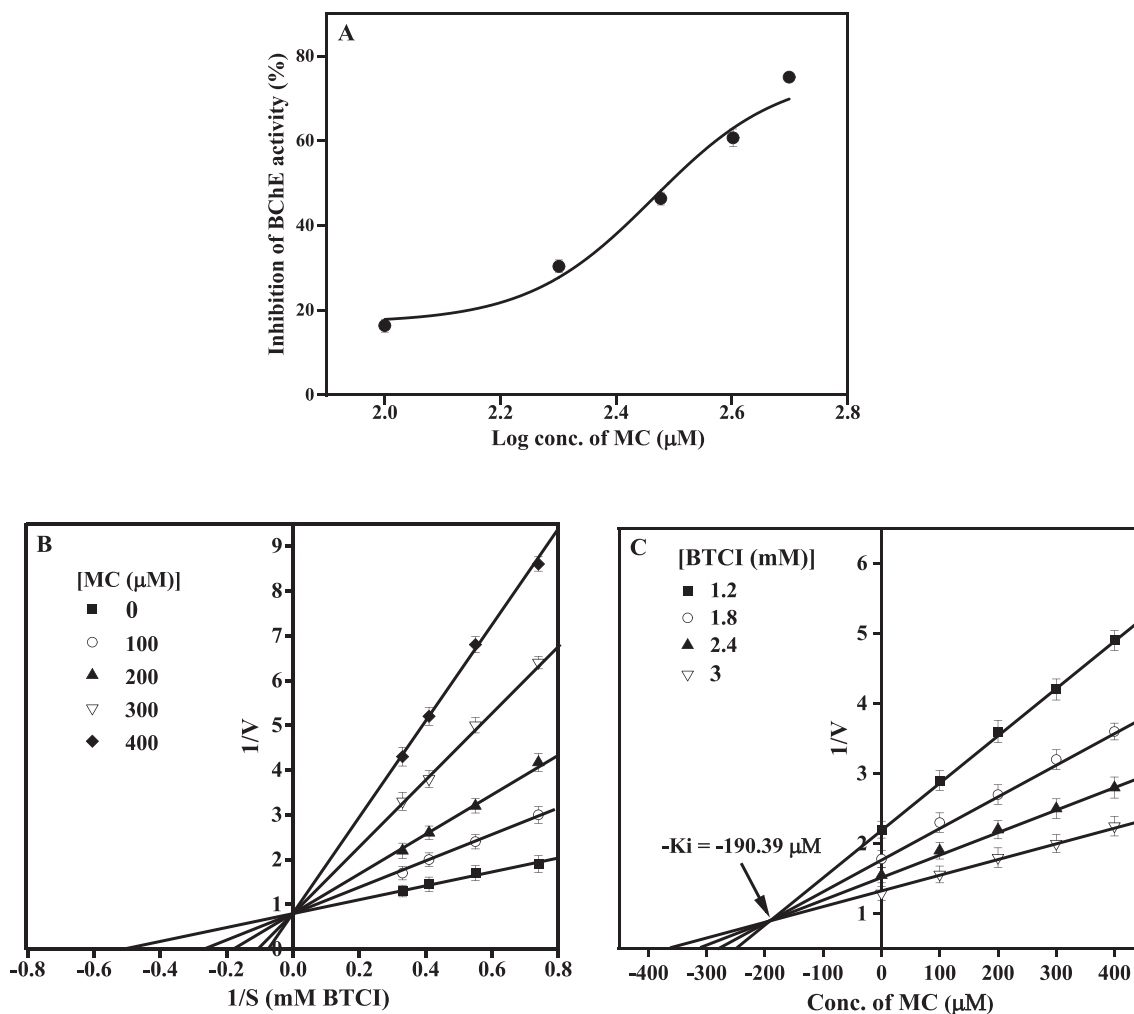
Fig. 6. MC effect on BChE enzyme activity. (A) Inhibition of BChE enzyme by MC. (B) LB plot showing inhibition type. (C) Dixon plot with Ki value of MC for BChE activity.

cients above 0.8 were depicted in dark cyan, indicating strong positive correlations, while residues with anti-correlated coefficients below < −0.4 were indicated in pale yellow. Percentage of pairwise correlated residues are found to be high which suggests a stable MC/AChE binding.

For the MC-BChE complex, the first seven eigenvectors demonstrated dominant movements with higher eigenvalues (26.3% to 58.7%), while subsequent eigenvectors showed no significant variations in the calculated eigen fraction from the seventh onward. The variability of PC1, PC2, and PC3 was 26.34%, 10.64%, and 6.76%, respectively (Fig. 11A). Similar to the MC-AChE complex, PC3 exhibited the most stable BChE/MC binding. It was observed that the total variance for the MC-AChE and MC-BChE complexes was 69.4% and 71.7%, respectively. This indicates that MC induced a higher motion of BChE Cα-atoms compared to AChE. The pairwise correlation map (DCCM map) demonstrated a high percentage of pairwise correlated residues between MC and the BChE protein, further confirming the stable binding of MC with BChE (Fig. 11B).

4. Discussion

AD is associated with a number of pathological characters such as oxidative stress, Aβ aggregation, deposit of tau protein, senile plaques and decreased level of cholinergic neurotransmitters (ACh). Currently available drugs for AD have numerous side-effects. Hence, it demands the identification of natural-based compounds to overcome AD. In recent years, medicinal plant concoction preparations or botanicals (plant materials applied in foods and food supplements) are preferred as complementary medicine because such preparation would have mixture of various bioactive phytochemicals. Different phytochemicals present in the extract would provide different beneficial effects such as direct therapeutic activity or reinforcement of the therapeutic potential of active principles present in the extract or might counteract the possible side-effects. Hence, the synergistic effect of these natural-compounds in an extract prepared from plant are considered advantageous (Durazzo et al., 2018). In accordance, *S. torvum* fruit is considered as an essential diet ingredient and a common vegetable in most of the countries (Darkwah et al., 2020). Hence, identifying the pharmacological properties (antioxidants and anticholinesterases activities) of *S. torvum* fruit and its principal active molecule MC would be advantageous in using it as botanicals for AD therapy.

4.1. Antioxidative effect of BESTF and MC

Redox imbalance causes damage to macromolecules which contribute to oxidative stress and results in impaired neuronal function in various neuronal degenerative disorder (Butterfield and Boyd-Kimball, 2018). Hence, the neutralization of reactive oxidants is the major target to prevent the oxidative stress. Number of medicinal plants and natural compounds isolated
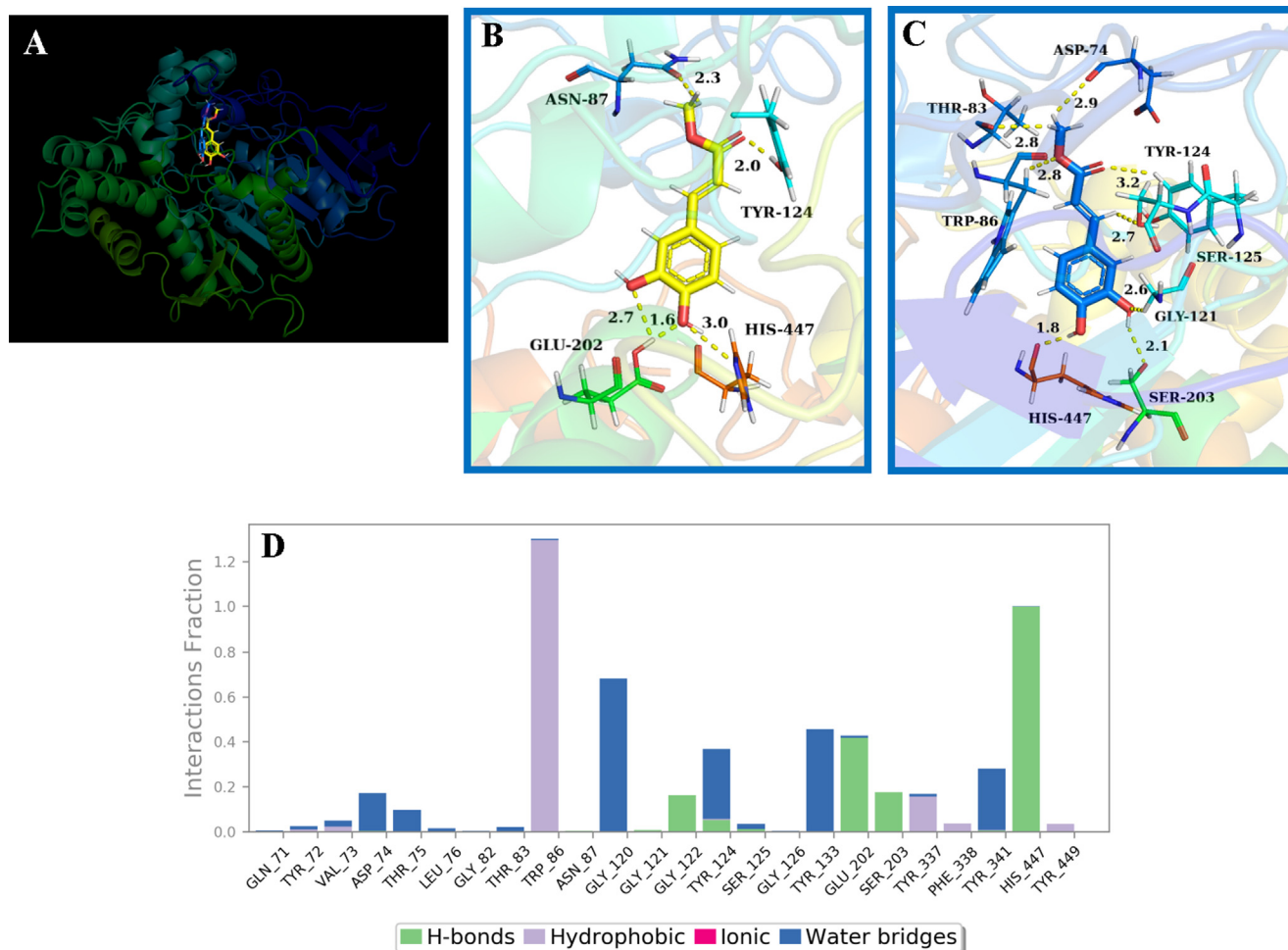
Fig. 7. Interaction of MC with AChE enzyme. (A) Superimposed surface figure showing the positioning of MC within active site gorge of AChE during docking and at the end of dynamics. Intermolecular interaction details of MC with active site amino acids of AChE at the end of docking (B) and at the end of 100 ns simulation (C). (D) The detail of AChE interacting amino acids with MC throughout the MD simulation.

Table 1
Details of interaction between methyl caffeate and amino acid present in human AChE and BChE.

Protein-ligand complex	Docking/MD	Interacting amino acid residues		
		Hydrogen bond	Hydrophobic interaction	Electrostatic interaction
AChE-MC	Docking	Trp86, Asn87, Tyr124, Glu202, Ser203	Gly120, Gly121	–
	MD	Asp74, Thr83, Trp86, Ser125, Ser203, His447	Val73, Trp86	–
BChE-MC	Docking	Tyr128, Glu197, Tyr332, Met437, His438	Trp82, Ala328	–
	MD	Gly116, Ser198, Ala328, His438, Gly439	Ala328, His438	Trp82

from these plants are used as potent antioxidants. In the present study, the extract prepared from *S. torvum* fruit contained many phytoconstituents such as phenols, flavonoids, saponins and tannins which might show many biological properties such as antimicrobial, antioxidant, antidiabetic, anti-inflammatory, nephroprotective, cardioprotective and neuroprotective effects (Darkwah et al., 2020). Due to presence of such phytoconstituents, BESTF showed scavenging activity against reactive oxidants (DPPH, ABTS and H_2O_2) and FRAP activity. Antioxidant act as a protector of brain against neuronal death which is associated with neuronal disorder (Ishige et al., 2001). Phytochemicals from *S. torvum* fruits are known for antioxidant effects (Darkwah et al., 2020). The aqueous extract of *S. torvum* inhibited the oxidative stress induced by cadmium (Ramamurthy et al., 2016). Similarly, BESTF showed better reducing potential against

FRAP assay which could be the results of the metal chelating property of *S. torvum*.

MC is considered the important biological active compound present in *S. torvum* fruit and widely studied for its biological effect (Shin et al., 2004; Takahashi et al., 2010; Balachandran et al., 2015). In line with this, MC showed significant *in vitro* antioxidant activity at low concentrations in the present study. *In silico* analysis has shown that MC through hydrogen atom transfer approach could have antioxidant effect (Urbaniak et al., 2017). Earlier investigations have demonstrated the neuroprotective benefits of *S. torvum* fruit extracts and MC against diverse oxidative stress conditions (Ishige et al., 2001; Mohan et al., 2017). Given the significant involvement of oxidative stress in cognitive impairment, the antioxidant attributes found in BESTF and MC could potentially contribute to their favorable impact on biological functions.
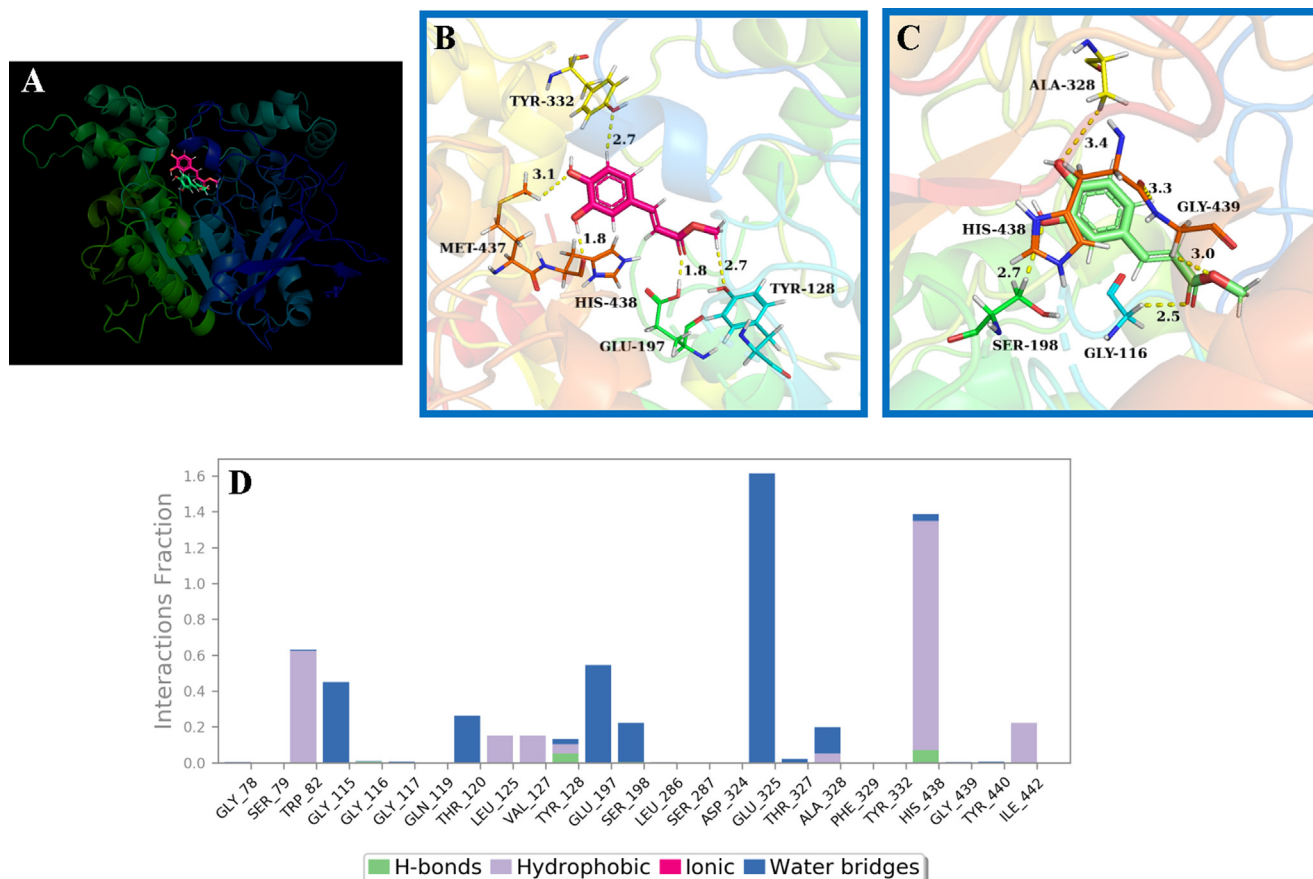
Fig. 8. Interaction of MC with BChE enzyme. (A) Superimposed surface figure showing the MC interaction with BChE active site gorge during docking and at the end of dynamics. Intermolecular interaction details of MC with BChE active site amino acid at the end of docking (B) and at the end of 100 ns MD simulation (C). (D) The detail of BChE interacting amino acids with MC throughout the MD simulation.

4.2. Inhibition of cholinesterases (AChE and BChE) by BESTF and MC

BESTF inhibited AChE and BChE at microgram per millilitre level. Presence of polyphenolic compounds in the *S. torvum* extract might be involved in the inhibition of AChE and BChE. Phenolic compounds such as rutoside, gallate, catechuic acid and 3,4-dihydroxycinnamic acid were found in methanolic extract of *S. torvum* which exhibited antidiabetic effect in diabetic rats (Gandhi et al., 2011). Similarly, various phenolic compounds are reported for its inhibitory effect against AChE and BChE (Murray et al., 2013). Various alkaloids such as tomatidine, tomantine, solasonine, and solanidine were found to be present in Solanum species (Senizza et al., 2021). The presence of alkaloids in Solanum might influence the inhibition of AChE and BChE, since alkaloids are known for cholinesterases inhibition (Santos et al., 2018). Phenolic acids such as hydroxycinnamic acid, hydroxybenzoic acid, vanillic acid, dihydroxycinnamic acid, cinnamic acids, 5-O-galloylquinic acid, syringic acid, *p*-goumaroyl tyrosine, 24-methyllathosterol ferulate, *p*-coumaroyl glucose are present in the Solanum species (Gandhi et al., 2011; Senizza et al., 2021). AChE inhibitory property was reported for phenolic acids namely, 2,5-dihydroxyphenylacetic acid, *p*-hydroxyphenylpyruvic acid, dihydronorguaiaretic acid, labiatenic acid, dihydroxycinnamic acid, gallate, 3-caffeoylquinic acid, vanillacetic acid and Sinapinic acid (Szwajgier, 2015). Hence, the inhibitory effect of MC against AChE and BChE which is found to be abundantly present in *S. torvum* fruit was studied.

MC inhibited both AChE and BChE in competitive manner at micromolar concentration. Inhibition of BChE was better in com-

parison to AChE by MC. The presence of caffeoyl group in MC might highly support in the inhibition of AChE and BChE. To support this notion, previous study reported that, 1,3,5-tri-O-caffeoyl quinic acid and 1,4,5-tri-O-caffeoyl quinic acid isolated from *Arctium lappa* L. root which contain three molecules of caffeoyl group in the structure act as strong neuronal protecting agent and inhibit neuronal apoptosis against H_2O_2-induced SH-SY5Y cells. Presence of more number and location of caffeoyl group determine the potential of the molecules (Gao et al., 2020). Compounds isolated from *Celastrus orbiculatus* such as caffeoyloxyfriedelin and caffeoyloxy-20β-hydroxyursane rather than celastrusin B which does not have caffeoyl moiety acted as better neuronal protecting agent against oxygen-glucose deprivation-induced SH-SY5Y cells damage (Li et al., 2016). Hence, the presence of caffeoyl group might play a vital function in neuronal protection against various toxicities. MC is known for mammalian alpha-glucosidase inhibition through which it could act as antidiabetic agent. It is imperative to note that, under diabetic conditions, cognitive impairment occurs due to degeneration of cholinergic neurotransmission therefore inhibition of cholinesterases is considered an important strategy to overcome cognitive decline (Loganathan et al., 2021). Also, association between AD and diabetes is suggested in humans. AChE and BChE levels are increased in the plasma of diabetic patients due to which ACh level is decreased and results in inflammation. Also, BChE causes insulin resistance and indirectly contributes to the pathogenesis of diabetes (Mushtaq et al., 2014). In such scenario, anticholinesterase effect of MC found in the present study shows that MC could be used for its dual effect as cognitive improvement activity and antidiabetic effect.
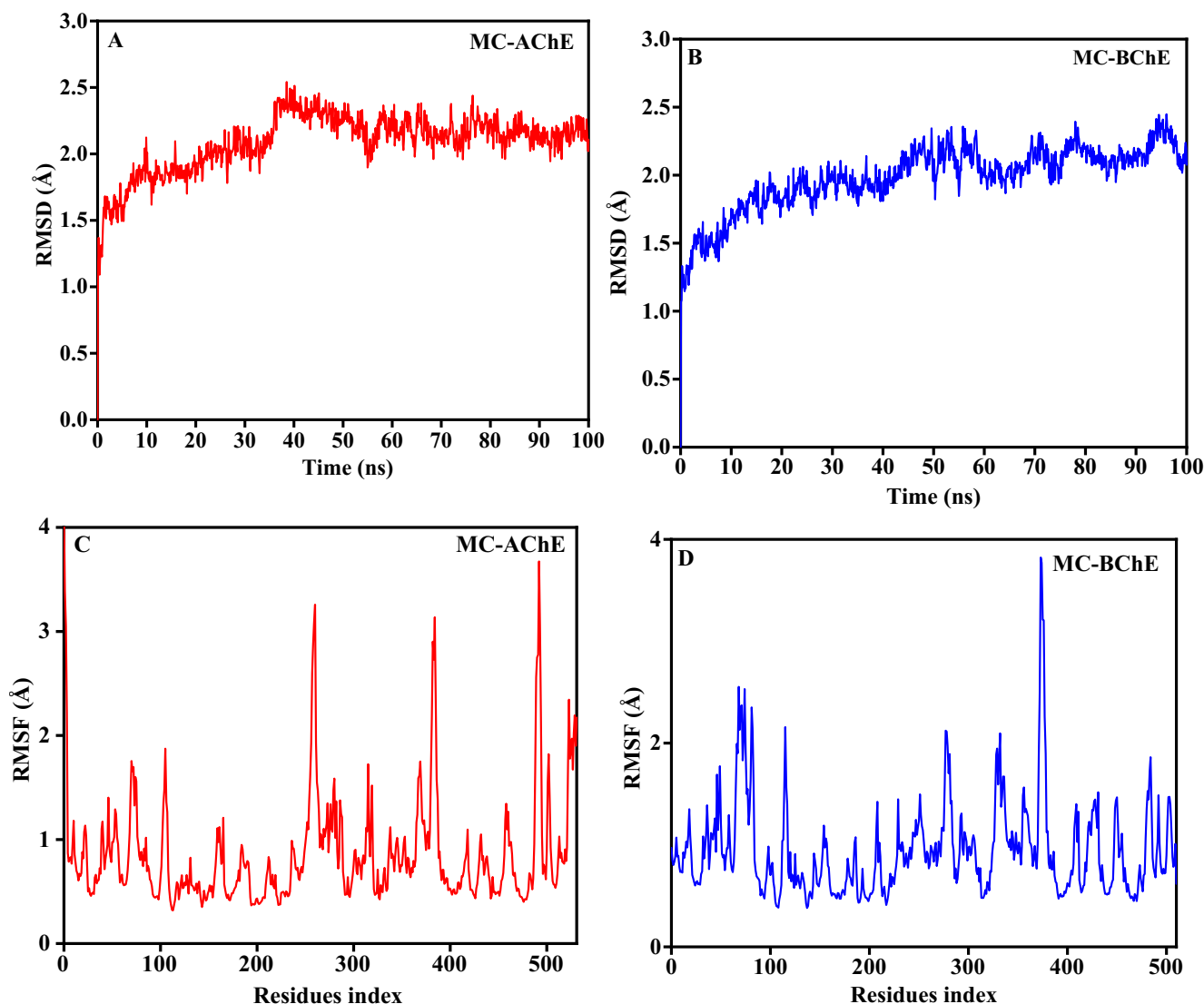
Fig. 9. (A and B) RMSD; (C and D) RMSF of AChE/MC and BChE/MC complexes.

Table 2
Binding free energy of MC interaction with AChE or BChE using Prime/MM-GBSA approach.

Protein	dG bind	Coulomb	Covalent	H bond	Lipo	vdW
	(kcal/mol)					
AChE	−41.85	−16.03	3.41	−0.52	−19.90	−30.95
BChE	−8.49	−8.16	10.06	−0.34	−18.85	−9.24

4.3. Molecular in-sight into the interaction of MC with AChE and BChE through in silico analysis

In consistent with the outcomes derived from the experimental study involving kinetic analysis and competitive inhibition, MC oriented within the active site gorge of these enzymes. Comprehensive analysis involving molecular docking and MD simulations corroborated this correlation, revealing interactions of MC with pivotal amino acids, including Ser125, Tyr124, and Asp74 of AChE. MC engaged with amino acids from the catalytic site and the peripheral anionic site (PAS), forming hydrogen and hydrophobic interactions with critical residues like Ser125, Tyr124, and Asp74

in AChE. Notably, hydrophobic interaction occurred with Trp86 situated within the AChE active site. Trp86 is crucial for stabilizing ACh in the catalytic site during the catalytic process, hence, interaction of MC with it would potentially impede substrate binding (Zhou et al., 2010). In the context of AChE-induced Aβ aggregation, which is linked to the PAS, MC's binding could hinder such aggregation similarly to other PAS-binding inhibitors like propidium, decamethonium, physostigmine and donepezil (Inestrosa et al., 1996; Bartolini et al., 2003). Similar to these PAS binding inhibitors, binding of MC in the PAS of AChE might hinder the AChE-induced Aβ aggregation. Phenolic compounds, excluding alkaloids, have been found to primarily interact with the PAS and anionic site of AChE and BChE. Consistently, the present study established MC's interaction with amino acids within these subsites (Santos et al., 2018). The stability of MC/AChE and MC/BChE complexes was supported by RMSD and RMSF values from MD simulations. Notably, the stable binding of MC with AChE or BChE stemmed from diverse factors, encompassing hydrogen bonding, Van der Waals force, lipophilic energy, and Coulomb's energy, as corroborated by MM/GBSA analysis. Further analysis, such as PCA and DCCM, indicated significant alterations in correlated motions and structural dynamics upon MC binding to AChE and BChE. Collectively, these findings
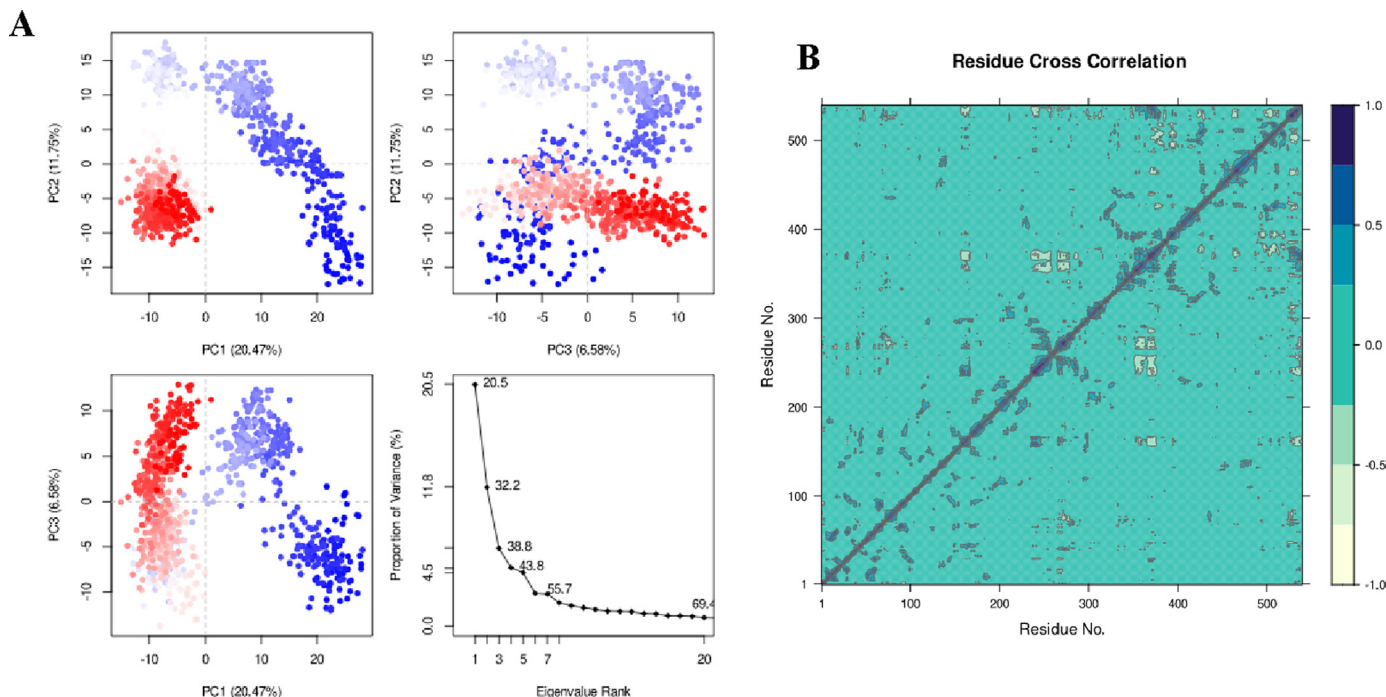
Fig. 10. PCA (A) and DCCM (B) analysis of MC/AChE complex. (A) The chart illustrates the distribution of variance percentage (% variance) in the MC-AChE complex across eigenvalues computed using PCA. Notably, three principal components (PCs) exhibit areas of fluctuation. The color spectrum, transitioning from blue to white to red, captures the periodic shifts observed over the 100 ns simulation. (B) The DCCM highlights the interactions within the MC-AChE complex. Strong positive correlations between residues are denoted by a dark blue shade, while weaker negative correlations are represented by a pale-yellow hue.
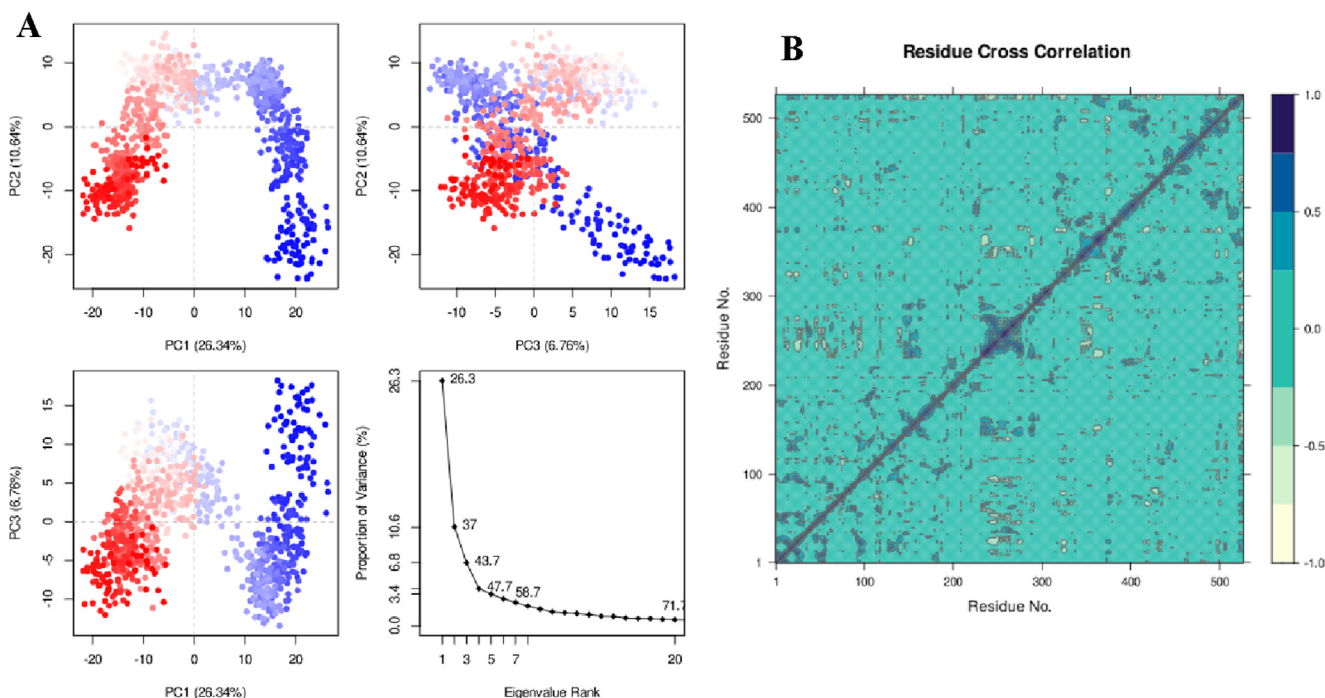
Fig. 11. PCA (A) and DCCM (B) analysis of MC/BChE complex. (A) The percentage variance in MC-BChE complex against eigenvalues computed by PCA. Periodic jump through simulation is given in transition from blue to white to red. (B) The DCCM map of MC-BChE complex. Dark blue: Positive correlation among the residues; Pale-yellow: Negative correlation.

underscore the efficient binding of MC with both AChE and BChE, shedding light on the multifaceted interactions that underlie this association.

5. Conclusion

Effective and safe (that do not elicit undesirable effects) inhibitors are being searched for cognitive improvement due to different

drawbacks presented with currently available therapies. Present study determined the anticholinesterase potential and antioxidants effect of BESTF and MC. BESTF showed potent *in vitro* antioxidant effect. BESTF inhibited AChE and BChE competitively. The presence of various phytochemicals in BESTF might have played synergetic effect in the antioxidant and enzymes inhibition potential. On the other hand, MC which is one of the phytochemicals present in *S. torvum* showed radical scavenging effects and cholinesterases (AChE and BChE) inhibitory effect. MC stably interacted in the AChE and BChE active site in *in silico*. Altogether, the results from the present study showed that BESTF and MC could be considered as botanicals or complementary medicine for treatment of cognitive impairment. Further, *in vivo* research is needed to explore the applicability of *S. torvum* fruit extract and MC for cognitive improvement.

Declaration of Competing Interest

The authors declare that they have no known competing financial interests or personal relationships that could have appeared to influence the work reported in this paper.

Acknowledgment

References

Al-Masri, A.A., Ameen, F., 2023. Anti-inflammatory effect of anthocyanin-rich extract from banana bract on lipopolysaccharide-stimulated raw 264.7 macrophages. J. Funct. Foods 107, 105628.

Balachandran, C., Emi, N., Arun, Y., Yamamoto, Y., Ahilan, B., Sangeetha, B., Duraipandiyan, V., Inaguma, Y., Okamoto, A., Ignacimuthu, S., 2015. *In vitro* anticancer activity of methyl caffeate isolated from solanum torvum swartz. Fruit. Chem. Biol. Interact. 242, 81–90.

Bartolini, M., Bertucci, C., Cavrini, V., Andrisano, V., 2003. Β-amyloid aggregation induced by human acetylcholinesterase: Inhibition studies. Biochem. Pharmacol. 65, 407–416.

Butterfield, D.A., Boyd-Kimball, D., 2018. Oxidative stress, amyloid-β peptide, and altered key molecular pathways in the pathogenesis and progression of alzheimer's disease. J. Alzheimers Dis. 62, 1345–1367.

Chen, Z.-R., Huang, J.-B., Yang, S.-L., Hong, F.-F., 2022. Role of cholinergic signaling in alzheimer's disease. Molecules 27, 1816.

Cheung, J., Rudolph, M.J., Burshteyn, F., Cassidy, M.S., Gary, E.N., Love, J., Franklin, M. C., Height, J.J., 2012. Structures of human acetylcholinesterase in complex with pharmacologically important ligands. J. Med. Chem. 55, 10282–10286.

Chitra, L., Penislusshiyan, S., Soundariya, M., Logeswari, S., Rajesh, R.V., Palvannan, T., 2022. Anti-acetylcholinesterase activity of *Corallocarpus epigaeus* tuber: *In vitro* kinetics, *in silico* docking and molecular dynamics analysis. J. Mol. Struc. 1255, 132450.

Darkwah, W.K., Koomson, D.A., Miwornunyuie, N., Nkoom, M., Puplampu, J.B., 2020. Phytochemistry and medicinal properties of *Solanum torvum* fruits. All Life. 13, 498–506.

Darvesh, S., 2016. Butyrylcholinesterase as a diagnostic and therapeutic target for alzheimer's disease. Curr. Alzheimer Res. 13, 1173–1177.

Dinamarca, M.C., Sagal, J.P., Quintanilla, R.A., Godoy, J.A., Arrázola, M.S., Inestrosa, N. C., 2010. Amyloid-β-acetylcholinesterase complexes potentiate neurodegenerative changes induced by the aβ peptide. Implications for the pathogenesis of alzheimer's disease. Mol. Neurodegener. 5, 1–15.

Dixon, M., 1953. The determination of enzyme inhibitor constants. Biochem. J. 55, 170.

Durazzo, A., D'Addezio, L., Camilli, E., Piccinelli, R., Turrini, A., Marletta, L., Marconi, S., Lucarini, M., Lisciani, S., Gabrielli, P., 2018. From plant compounds to botanicals and back: A current snapshot. Molecules 23, 1844.

Galvão, M.A.M., Arruda, A.O.D., Bezerra, I.C.F., Ferreira, M.R.A., Soares, L.A.L., 2018. Evaluation of the folin-ciocalteu method and quantification of total tannins in stem barks and pods from libidibia ferrea (mart. Ex tul) lp queiroz. Braz. Arch. Biol. Technol. 61.

Gandhi, G.R., Ignacimuthu, S., Paulraj, M.G., 2011a. Solanum torvum swartz. Fruit containing phenolic compounds shows antidiabetic and antioxidant effects in streptozotocin induced diabetic rats. Food Chem. Toxicol. 49, 2725–2733.

Gandhi, G.R., Ignacimuthu, S., Paulraj, M.G., Sasikumar, P., 2011b. Antihyperglycemic activity and antidiabetic effect of methyl caffeate isolated

from solanum torvum swartz. Fruit in streptozotocin induced diabetic rats. Eur. J. Pharmacol. 670, 623–631.

Gao, H., Jiang, X.-W., Yang, Y., Liu, W.-W., Xu, Z.-H., Zhao, Q.-C.-J.-P., 2020. Isolation, structure elucidation and neuroprotective effects of caffeoylquinic acid derivatives from the roots of *Arctium lappa* L. Phytochemistry 177, 112432.

Hiai, S., Oura, H., Nakajima, T., 1976. Color reaction of some sapogenins and saponins with vanillin and sulfur1c acid. Planta Med. 29, 116–122.

Inestrosa, N.C., Alvarez, A., Perez, C.A., Moreno, R.D., Vicente, M., Linker, C., Casanueva, O.I., Soto, C., Garrido, J., 1996. Acetylcholinesterase accelerates assembly of amyloid-β-peptides into alzheimer's fibrils: Possible role of the peripheral site of the enzyme. Neuron 16, 881–891.

Ishige, K., Schubert, D., Sagara, Y., 2001. Flavonoids protect neuronal cells from oxidative stress by three distinct mechanisms. Free Radic. Biol. Med. 30, 433–446.

Li, J.-L., Wu, L., Wu, J., Feng, H.-X., Wang, H.-M., Fu, Y., Zhang, R.-J., Zhang, H.-Y., Zhao, W., 2016. Caffeoyl triterpenoid esters as potential anti-ischemic stroke agents from *Celastrus orbiculatus*. J. Nat. Prod. 79, 2774–2779.

Lineweaver, H., Burk, D., 1934. The determination of enzyme dissociation constants. J. Am. Chem. Soc. 56, 658–666.

Loganathan, C., Sakayanathan, P., Thayumanavan, P., 2021. Astaxanthin-s-allyl cysteine diester against high glucose-induced neuronal toxicity in vitro and diabetes-associated cognitive decline in vivo: Effect on p53, oxidative stress and mitochondrial function. Neurotoxicology 86, 114–124.

Marucci, G., Buccioni, M., Dal Ben, D., Lambertucci, C., Volpini, R., Amenta, F., 2021. Efficacy of acetylcholinesterase inhibitors in alzheimer's disease. Neuropharmacol. 190, 108352.

Mohan, M., Gangurde, S., Kadam, V., 2017. Protective effect of *Solanum torvum* on monosodium glutamate-induced neurotoxicity in mice. Indian J. Nat. Prod. Resour. 8, 351–359.

Murray, A.P., Faraoni, M.B., Castro, M.J., Alza, N.P., Cavallaro, V., 2013. Natural ache inhibitors from plants and their contribution to alzheimer's disease therapy. Curr. Neuropharmacol. 11, 388–413.

Mushtaq, G., Greig, N.H., Khan, J.A., Kamal, A.M., 2014. Status of acetylcholinesterase and butyrylcholinesterase in Alzheimer's disease and type 2 diabetes mellitus. CNS Neurol. Disord. Drug Targets 13, 1432–1439.

Nicolet, Y., Lockridge, O., Masson, P., Fontecilla-Camps, J.C., Nachon, F., 2003. Crystal structure of human butyrylcholinesterase and of its complexes with substrate and products. J. Biol. Chem. 278, 41141–41147.

Patel, S.S., Raghuwanshi, R., Masood, M., Acharya, A., Jain, S.K., 2018. Medicinal plants with acetylcholinesterase inhibitory activity. Rev. Neurosci. 29, 491–529.

Pavithra, K., Vadivukkarasi, S., 2015. Evaluation of free radical scavenging activity of various extracts of leaves from Kedrostis foetidissima (jacq.) cogn. Food Sci. Hum. Wellness. 4, 42–46.

Ramamurthy, C., Subastri, A., Suyavaran, A., Subbaiah, K., Valluru, L., Thirunavukkarasu, C., 2016. *Solanum torvum swartz*. Fruit attenuates cadmium-induced liver and kidney damage through modulation of oxidative stress and glycosylation. Environ. Sci. Pollut. Res. 23, 7919–7929.

Roe, D.R., Cheatham, T.E., 2013. Ptraj and cpptraj: Software for processing and analysis of molecular dynamics trajectory data. J. Chem. Theory Comput. 9, 3084–3095.

Sakayanathan, P., Loganathan, C., Kandasamy, S., Ramanna, R.V., Poomani, K., Thayumanavan, P., 2019. *In vitro* and *in silico* analysis of novel astaxanthin-s-allyl cysteine as an inhibitor of butyrylcholinesterase and various globular forms of acetylcholinesterases. Int. J. Biol. Macromol. 140, 1147–1157.

Sani, S., Lawal, B., Ejeje, J.N., Aliu, T.B., Onikanni, A.S., Uchewa, O.O., Ovoh, J.C., Ekpa, F.U., Ozoagu, C.D., Akuma, T.S., 2022. Biochemical and tissue physiopathological evaluation of the preclinical efficacy of Solanum torvum swartz leaves for treating oxidative impairment in rats administered a β-cell-toxicant (stz). Biomed. Pharmacother. 154, 113605.

Santos, T.C.D., Gomes, T.M., Pinto, B.A.S., Camara, A.L., Paes, A.M.D.A., 2018. Naturally occurring acetylcholinesterase inhibitors and their potential use for Alzheimer's disease therapy. Front. Pharmacol. 9, 1192.

Senizza, B., Rocchetti, G., Sinan, K.I., Zengin, G., Mahomoodally, M.F., Glamocilja, J., Sokovic, M., Lobine, D., Etienne, O.K., Lucini, L., 2021. The phenolic and alkaloid profiles of *Solanum erianthum* and *Solanum torvum* modulated their biological properties. Food Biosci. 41, 100974.

Shin, K.-M., Kim, I.-T., Park, Y.-M., Ha, J., Choi, J.-W., Park, H.-J., Lee, Y.S., Lee, K.-T., 2004. Anti-inflammatory effect of caffeic acid methyl ester and its mode of action through the inhibition of prostaglandin e2, nitric oxide and tumor necrosis factor-α production. Biochem. Pharmacol. 68, 2327–2336.

Szwajgier, D., 2015. Anticholinesterase activity of selected phenolic acids and flavonoids-interaction testing in model solutions. Ann. Agric. Environ. Med. 22, 690–694.

Takahashi, K., Yoshioka, Y., Kato, E., Katsuki, S., Iida, O., Hosokawa, K., Kawabata, J., 2010. Methyl caffeate as an α-glucosidase inhibitor from solanum torvum fruits and the activity of related compounds. Biosci. Biotech. Bioch. 74, 741–745.

Urbaniak, A., Kujawski, J., Czaja, K., Szelag, M., 2017. Antioxidant properties of several caffeic acid derivatives: A theoretical study. C. R. Chim. 20, 1072–1082.

Yiannopoulou, K.G., Papageorgiou, S.G., 2020. Current and future treatments in alzheimer disease: An update. J. Cent. Nerv. Syst. Dis. 12. 1179573520907397.

Zhou, Y., Wang, S., Zhang, Y., 2010. Catalytic Reaction Mechanism of Acetylcholinesterase Determined by Born-Oppenheimer Ab Initio QM/MM Molecular Dynamics Simulations. J. Phys. Chem. B. 114, 8817–8825.